

# Growth Deceleration of Vertically Aligned Carbon Nanotube Arrays: Catalyst Deactivation or Feedstock Diffusion Controlled?

*Rong Xiang<sup>a,b</sup>, Zhou Yang<sup>b</sup>, Qiang Zhang<sup>b</sup>, Guohua Luo<sup>b</sup>, Weizhong Qian<sup>b</sup>, Fei Wei<sup>b\*</sup>, Masayuki Kadowaki<sup>a</sup>, Erik Einarsson<sup>a</sup>, Shigeo Maruyama<sup>a\*</sup>*

<sup>a</sup>Department of Mechanical Engineering, The University of Tokyo,  
7-3-1 Hongo, Bunkyo-ku, Tokyo 113-8656, Japan

<sup>b</sup>Beijing Key Laboratory of Green Chemical Reaction Engineering and Technology,  
Department of Chemical Engineering, Tsinghua University, Beijing 100084, China

## ABSTRACT

Feedstock and byproduct diffusion in the root growth of aligned carbon nanotube arrays is discussed. A non-dimensional modulus is proposed to differentiate catalyst-poisoning controlled growth deceleration from one which is diffusion controlled. It is found that, at current stage, aligned multi-walled carbon nanotube arrays are usually free of feedstock diffusion resistance while single-walled carbon nanotube arrays are already suffering from a strong diffusion resistance. The method presented here is also able to predict the critical lengths in different CVD processes from which carbon nanotube arrays begin to meet strong diffusion resistance, as well as the possible solutions to this diffusion caused growth deceleration.

---

\* To whom correspondence should be addressed.

Fei Wei, [weifei@flotu.org](mailto:weifei@flotu.org), Department of Chemical Engineering, Tsinghua University, Beijing 100084, China; tel, 86-10-62788984; fax, 86-10-62772051.

Shigeo Maruyama, [maruyama@photon.t.u-tokyo.ac.jp](mailto:maruyama@photon.t.u-tokyo.ac.jp), Department of Mechanical Engineering, The University of Tokyo, 7-3-1 Hongo, Bunkyo-ku, Tokyo 113-8656, Japan; tel, 81-3-5841-6421; fax, 81-3-5800-6983.

Vertically aligned carbon nanotube (CNT) arrays grown on flat substrates<sup>1-7</sup>, in which all the nanotubes are of similar orientation and length, offer an ideal platform to study CNT growth mechanisms and kinetics. Since 1996<sup>1</sup>, various chemical vapor deposition (CVD) methods, including floating catalytic CVD<sup>2</sup>, plasma enhanced CVD<sup>3</sup> and thermal CVD<sup>4</sup> have been proposed to synthesize aligned multi-walled carbon nanotube (MWNT) arrays. Lately, alcohol catalytic CVD<sup>5</sup> (ACCVD), water assisted CVD<sup>6</sup>, microwave plasma CVD<sup>7</sup>, etc. are used to produce vertically aligned single-walled carbon nanotube (SWNT) arrays. These processes usually involve different catalysts, carbon sources and operation parameters, resulting in products with different morphologies and qualities. However, none of these CNT growth processes can overcome the gradual deceleration and eventual termination of growth. The ability to understand and thereby to overcome the underlying deactivation mechanisms becomes one of the most critical steps to develop nano-scale tubes into real macroscopic materials.

Recently, many groups have affirmed the root growth mode of their vertically aligned CNTs, indicating that the feedstock molecules have to diffuse through the thick CNT array, reach the substrate where catalysts are located, and then contribute to the CNT growth.<sup>8-13</sup> In this bottom-up growth process, the diffusion resistance of the feedstock from the top to the root arises as an obstruction, and can act as a unique decelerating growth mechanism. Existence of a feedstock diffusion resistance means that concentration of the carbon source at the CNT root should be lower than the bulk concentration. Previously, Zhu et al.<sup>14</sup> fitted experimentally-obtained film thicknesses with the square root of growth time, and stated that the growth deceleration is attributed to the strong diffusion limit of feedstock to the CNT root. However, Hart et al.<sup>15</sup> claimed later that their growth curve can be accurately described by either diffusion limit or catalyst deactivation, suggesting that only fitting is not sufficient to clarify a diffusion controlled process from a catalyst deactivation controlled (catalyst decay) one. Furthermore, if the process is in the transition region, i.e. not completely diffusion controlled, root square fitting is no longer available. Here, we propose a method of using a non-dimensional modulus to quantitatively evaluate the degree of feedstock diffusion resistance (no diffusion resistance regime, transient regime, and strong diffusion limit regime). ACCVD<sup>16</sup> grown single-walled carbon nanotubes (SWNTs)<sup>5,17-20</sup> were used as a typical example of this method, and were found to be essentially free of feedstock diffusion resistance. The byproduct back diffusion<sup>19</sup>, which has never been taken into account previously, can also be estimated by the present method. Considering the similar diffusion behavior in different CVD processes, five of the most frequently used systems are also discussed. The results agree well with the currently available experimental results.

Vertically aligned SWNTs were synthesized on Co/Mo dip-coated<sup>21</sup> quartz substrates at 800 °C from ethanol as a carbon source. MWNT arrays were grown on quartz substrates at 800 °C with simultaneous feeding of cyclohexane and ferrocene<sup>22</sup>. Details of the growth

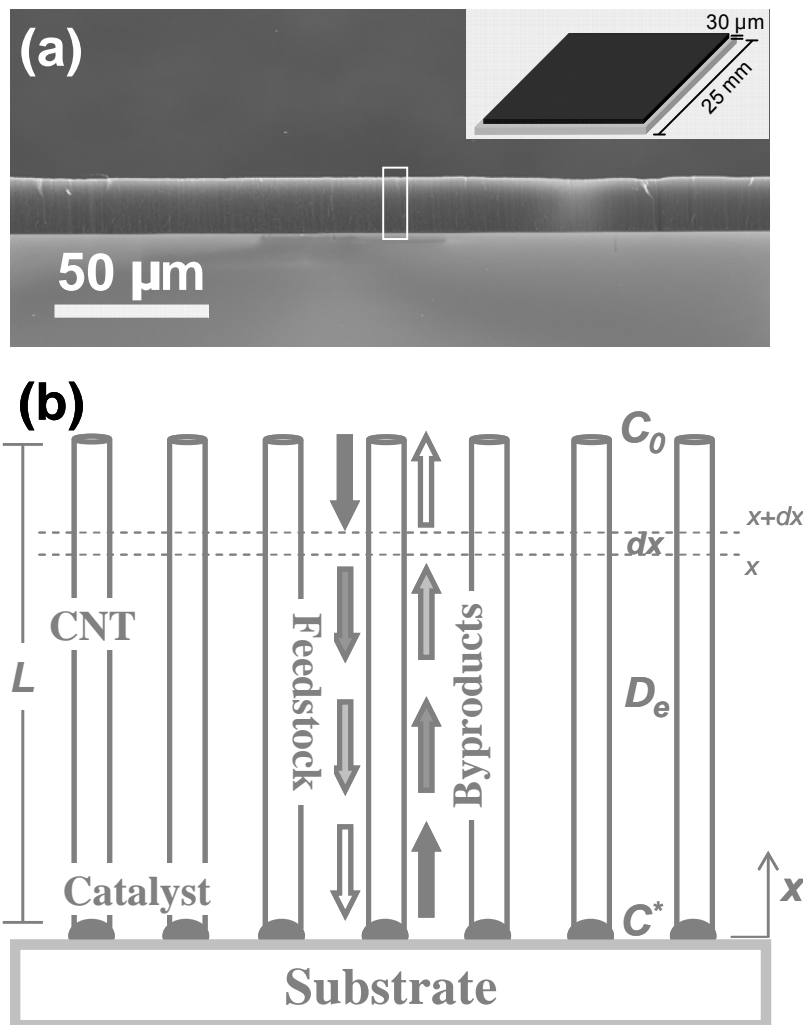


Figure 1. (a) SEM micrograph of vertically aligned SWNT arrays from ACCVD, inset at top-right is a schematic of a CNT film on substrate, suggesting the different dimensions of film size and thickness; (b) schematic presentation describing the diffusion of feedstock as well as gas product during the root growth of CNT arrays.

processes can be found in our previous work.<sup>17,22</sup> The lengths of as-grown CNT arrays were measured by SEM (JSM-7000 and JSM-7401), and average diameters were determined by TEM (JOEL 2010).

First, it is worth clarifying the concept of diffusion limit that is to be discussed below. Figure 1 presents the root growth process of aligned CNT arrays. As carbon source is being decomposed and extruded into solid CNT on catalyst. The concentration of feedstock molecules (e.g. ethanol in ACCVD) at the CNT root, which chemically determined the reaction rate, will be much lower than top (bulk concentration) if feedstock molecules are not diffusing fast enough from top to

root. Similarly, if the byproduct molecules generated by CNT growth can not diffuse fast, their concentration will also be higher at CNT root than near the top. This concentration difference at the root and top of a CNT array is the origin of diffusion limit. Other facts, such as catalyst oxidation, aggregation, reaction with substrate, formation of amorphous soot or graphitic structure covered on catalyst particles, are attributed to the catalyst poisoning (causing smaller  $k_s$  as to be discussed later), although some of them, e.g. soot formation, also prohibit carbon source from reaching catalyst. Also, we only consider one-dimensional diffusion (along the tube axis) inside CNT array. The diffusion from the sides of the forest is neglected because of the following two reasons. First, the side diffusion distance, i.e. the width of the vertically aligned CNT film ( $\sim 25$  mm) is usually much larger than the top diffusion distance, i.e. the film thickness (usually several millimeters at most). Second, side diffusion is probably more difficult due to the higher collision frequency in the anisotropic structure of the vertically aligned CNT array. Therefore, in a small sliced CNT array region  $dx$  (as indicated by dashed lines in Fig.1b), the difference in the amount of feedstock diffusing in from the top and diffusing out from the bottom should be what is consumed inside this  $dx$  region. At CNT-substrate interface, although microscopically (at molecular level) not all collisions between feedstock molecule and catalyst can result in CNT growth, the macroscopic net diffusion flux equals to the CNT formation rate (either expressed by the reaction rate  $k_s SC^{*m}$  or the macroscopic growth rate  $aS dL/dt$ ) when in equilibrium. Following basic diffusion theory, Fick's Law (diffusion flux is proportional to concentration gradient), and reaction theory<sup>23</sup>, this process can be expressed by

$$D_e S \left( \frac{dC}{dx} \right)_{x+dx} - D_e S \left( \frac{dC}{dx} \right)_x = 0 \quad (\text{inside of CNT forest}), \quad (1)$$

and

$$D_e S \left( \frac{dC}{dx} \right)_{x=0} = k_s SC^{*m} = aS \frac{dL}{dt} \quad (\text{root of CNT forest}), \quad (2)$$

where  $D_e$  is the effective diffusion coefficient,  $S$  film area,  $x$  normal coordinate from substrate,  $L$  length of CNT array,  $k_s$  surface reaction constant of carbon source to CNT,  $C^*$  effective feedstock concentration at the CNT root,  $m$  reaction order, and  $a$  structure-dependent constant of CNT array. Here, we emphasize that, although CNT growth can be divided into detailed steps, i.e. first feedstock decomposition, then carbon diffusion inside metal and final carbon precipitation, all these steps are treated as together here and  $k_s$  is the reaction constant of the overall process from carbon source to CNTs. In other words,  $k_s$  represents the dependence of overall CNT growth rate on carbon source concentration. This is also the only growth constant that we can obtain directly from experiments. Equation (1) is solved as  $\frac{d^2C}{dx^2} = 0$  or  $\frac{dC}{dx} = \text{const}$  and means that the feedstock concentration is linearly decreasing from top to root, thus, equation (2) can be modified to

$$D_e S \frac{C_0 - C^*}{L} = k_s S C^{*m} = a S \frac{dL}{dt}. \quad (3)$$

Therefore, as soon as we know the reaction order  $m$  and the reaction coefficient  $k_s$ , the effective concentration  $C^*$  can be found from equation (3), and then the time-dependent growth curve can be determined from an integration of equation (3).

Experiments were carried out under different ethanol pressures to investigate the growth order in the ACCVD method. It is found that the initial growth rate is almost proportional to the ethanol concentration<sup>20</sup> (see supporting information), suggesting  $m = 1$ , which is also found to be approximately valid in other processes (e.g. for water assisted super growth<sup>24</sup>). If  $k_s$  can be constant, the effective concentration  $C^*$  is calculated as  $C^* = \frac{D_e C_0}{D_e + L k_s}$ . Then, equation (3)

becomes

$$a \frac{dL}{dt} = k_s C^* = k_s \frac{D_e C_0}{D_e + L k_s} \quad (4)$$

By integrating equation (4), time-dependent growth curve is deduced as

$$L = \sqrt{\left(\frac{D_e}{k_s}\right)^2 + \frac{2D_e C_0}{a} t} - \frac{D_e}{k_s}. \quad (5)$$

This equation can be proportional to either  $t$  (no diffusion limit) or  $t^{1/2}$  (strong diffusion limit), depending on the values of  $\frac{2D_e C_0}{a} t$  and  $\frac{D_e}{k_s}$  (see supporting information). It is similar to what is widely used in silicon oxidation, the so-called ‘‘Deal-Grove’’ relationship<sup>25</sup>, as discussed previously.<sup>14, 26</sup> One can, in principle, also predict the growth curve of a CNT array provided that all the parameters listed above are known. However, a big difference between growth of a CNT array and silicon oxide is that, in most cases, the catalyst for CNT growth undergoes catalyst poisoning. Therefore,  $k_s$  in CNT growth is also a time-dependent parameter, unlike in silicon oxidation, where  $k_s$  is constant. This means that equation (5) only predict the ideal growth curve where catalyst activity does not decay.

To enable a simple estimate on the existence of a diffusion limit for a certain system and CNT length, we can define a non-dimensional number  $\varphi$  by

$$\varphi = \frac{k_s L}{D_e}. \quad (6)$$

This number represents physically the ratio of catalytic capability to diffusive capability. Then, the ratio of effective concentration to bulk concentration,  $\eta$  (usually called the effective factor) can be correlated with  $\varphi$  via a simple function from equation (3) as

$$\eta = \frac{C^*}{C_0} = \frac{D_e}{k_s L + D_e} = \frac{1}{\varphi + 1}. \quad (7)$$

This factor allows us to quantitatively characterize the degree of the diffusion limit. When  $\varphi$  is small (e.g.  $<0.1$ ), it is much easier to diffuse than to react, thus the effective factor will be nearly 1 ( $\eta > 0.9$ ), indicating there is little diffusion resistance. In contrast, when  $\varphi$  is large (e.g.  $>9$ ), it is more difficult to diffuse than to react, thus the effective factor  $\eta$  will be nearly zero ( $<0.1$ ) and the overall reaction will be dominated by the diffusion rate. The in-between situation is what we mentioned before as the transition regime, where the growth curve will be proportional to neither  $t$  nor  $t^{1/2}$ .

In ACCVD synthesis, the carbon feedstock at top of the SWNT array is constantly refreshed, and therefore the byproduct concentration can be treated as zero due to the high ethanol flow rate. Thus if we assume that one  $C_2H_5OH$  molecule produces one byproduct molecule, e.g.  $H_2O$  or  $H_2$ , after decomposition ( $A \rightarrow CNT + B + \dots$ ), the byproduct concentration at the CNT root can be also revealed as a single function of  $\varphi$ ,

$$C_B^* = C_0 \times \sqrt{\frac{M_B}{M_A}} \times \left( \frac{\varphi}{\varphi + 1} \right). \quad (8)$$

According to the above discussion, as long as we know  $D_e$  and  $k_s$ , the influence of diffusion can be concluded simply from the value of  $\varphi$  for a certain CNT length  $L$ . We know that the average diameter of SWNTs produced by ACCVD is about 2 nm, and the density of the as-grown film is about  $0.04 \text{ g/cm}^3$ . Therefore, the average distance between adjacent SWNTs can be easily calculated to be 8.8 nm. As the mean free path of ethanol in this process is about 16000 nm, much larger than the distance between SWNTs, it can be concluded that the ethanol diffusion resistance is mainly due to the ethanol-CNT collisions, i.e. in the range of Knudsen diffusion. Thereby, the diffusion coefficient can be estimated from collision theory if assuming CNT tortuosity as diffusion channel tortuosity<sup>27</sup>. As for  $k_s$ , we can use the initial value at  $t=0$  when the CNT growth is free of diffusion resistance. With the estimated  $D_e$  and experiment-derived  $k_s$ ,  $\varphi$  is calculated to be 0.054 ( $\ll 1$ ) for 30  $\mu\text{m}$  SWNT arrays in ACCVD. This means the ethanol concentration at the CNT root, where the catalyst is located, is almost the same as the concentration at the CNT top (95% from equation (7)). The vertical distribution of ethanol concentration in the array is plotted in Fig. 2a as A-SWNT. Thus, this process is catalyst deactivation controlled rather than diffusion controlled. After we peel the as-grown film off the substrate, most of the catalysts remain on the substrate, but the substrate is not active for a second growth. This confirmed that the catalyst poisoning contributed to the growth deceleration, which agrees with above calculation of  $\varphi$ . We know  $H_2O$  is a byproduct of ethanol decomposition, estimating through equation (8) reveals the concentration of water at the CNT root is several hundred ppm. Considering the previous report on the critical role of  $H_2O$  or  $O_2$  on

the growth of SWNT<sup>6, 16, 28</sup>, we plot the concentration distribution of H<sub>2</sub>O in Fig. 2a. This result is interesting, but currently we are not sure if this water concentration is critical for successful SWNT nucleation, or its relation to catalyst deactivation in ACCVD. Further work is needed in this area.

One may notice the above discussion on the feedstock diffusion is versatile and valid for all the first-order growth methods of aligned CNTs, applying to both SWNTs and MWNTs. Therefore, with the available data in the literature, we are able to estimate the degree of diffusion resistance in other CVD processes used to grow aligned CNT forests. The only difference here is when estimating the effective diffusion coefficient for MWNT arrays, the molecular diffusion should also be taken into account because the mean free path is comparable to the inter-tube distance for MWNT arrays, as listed in Tab. 1.

We analyzed four other CVD processes: a 2 mm MWNT array by floating CVD<sup>22, 29-31</sup> (F-MWNT), a 2.5mm SWNT array by super growth by Hata et al.<sup>6, 24, 32</sup> (S-SWNT), a 2.5 mm SWNT array by microwave plasma CVD by Zhong et al.<sup>7, 26, 33</sup> (P-SWNT), and a 400  $\mu\text{m}$  MWNT by thermal CVD by Zhu et al.<sup>11, 14, 34</sup> (T-MWNT). The results are compared with our 30  $\mu\text{m}$  SWNT array produced by ACCVD (A-SWNT) in Table 1. It can be seen that,  $k_s$  and  $D_e$ , the two key parameters to determine  $\varphi$ , and thus the degree of diffusion difficulty, have quite large difference among various CVD processes, especially between SWNT and MWNT arrays.  $D_e$  in SWNTs is usually one order of magnitude lower than that in MWNT because SWNTs are much more densely packed than MWNT (the inter-tube distance is smaller). Reaction constants are obtained experimentally from equation  $r=k_sSC$ . Larger  $k_s$  for SWNT growth is due to the lower carbon source concentration ( $C$ ) but similar CNT growth rate ( $r$ ). One possible physical reason for this difference in growth constant might be the higher catalytic activity for smaller metal particles in absorbing and decomposing hydrocarbon molecules. Because of these differences, it is suggested that, for mm-scale SWNTs,  $\varphi$  is usually much larger than 1 and, even if there is no catalyst poisoning, the growth rate of mm-scale SWNT arrays will still drop to only 10% due to the strong feedstock diffusion resistance. However, as the concentration at the root of array is of little difference from the bulk concentration, above 90%, even when there is no catalyst deactivation (if considering a decrease of  $k_s$  in real systems, the concentration would be higher), the diffusion resistance seems to not be the dominant reason for the decreasing growth in MWNT arrays. The feedstock concentration distribution in these CNT arrays is presented in Fig. 2a. As the  $\varphi$  is simply  $L$  dependent, we can also predict the critical length, as shown in Fig. 2b, above which diffusion problem begins to take an effect. It seems we might not need to worry about diffusion resistance for MWNTs before we can grow almost 10 cm to 1 m high CNT arrays, unless the diffusion phenomenon inside a CNT array is much different from classic Knudsen theory.

Table 1. System parameters and as-calculated  $\varphi$  and  $\eta$ .

Parameters	Abb.	Unit	A-SWNT	S-SWNT	P-SWNT	T-MWNT	F-MWNT
Temperature	$T$	(K)	1073	1023	873	1023	1073
Molecular weight	$M$	(-)	46	28	16	28	84
Density	-	(g/cm	0.041	0.037	0.067	0.014	0.082
CNT Diameter	-	(nm)	2	3	2	10	29
Number density	-	(m <sup>-2</sup> )	8.5E15	5.2E15	1.4E16	3E14	2.1E13
Porosity	$\rho$	(-)	0.973	0.963	0.956	0.976	0.986
Inter-tube distance	-	(nm)	8.8	10.9	6.5	48	189
Mean free path	$\lambda$	(nm)	16000	206	5500	196	91
Growth rate	-	(m/s)	2E-7	3.75E-6	5E-8	1.2E-6	5E-7
Reaction constant	$k_s$	(m/s)	2.4E-3	9.2E-3	5.7E-3	1.2E-4	3.5E-4
Diffusion coefficient	$D_e$	(cm <sup>2</sup> /	0.013	0.020	0.015	0.085	0.169
Length	$L$	(mm)	0.03	2.5	2.5	0.4	2
Proposed number	$\varphi$	(-)	0.054	11.3	9.7	0.0057	0.042
Effective factor	$\eta$	(-)	0.949	0.081	0.093	0.994	0.960

From equation (6), the influences of different parameters on the diffusion behavior can be investigated, and strategies to overcome the diffusion limit for the SWNT growth can also be revealed. Increasing  $D_e$  and decreasing  $k_s$  or  $L$  are all possible ways to decrease  $\varphi$ . However, the influences of these parameters are very limited because to bring diffusion limited processes to the reaction controlled region one usually needs to decrease  $\varphi$  by two orders of magnitude, as expressed in Equation (7). One promising approach is to pattern the continuous CNT film into pillar-like or sheet-like micron structure to allow easy side diffusion, as demonstrated by Zhong et al.<sup>26</sup> However, we found this strategy didn't work for our F-MWNT in yielding longer CNT arrays.<sup>30</sup> This means there exists strong diffusion resistance in P-SWNT but not in F-MWNT, which agrees well with the above calculated results on these two situations. One may also notice the edge of the CNT arrays produced by the "super growth" method is usually higher than the center part of the array. This might also be an evidence for the diffusion limit in this process. Besides Zhong's strategy, gradually increasing the feedstock partial pressure during the growth so as to keep the effective concentration at the CNT root constant might be another way to overcome this diffusion limit caused growth decay.

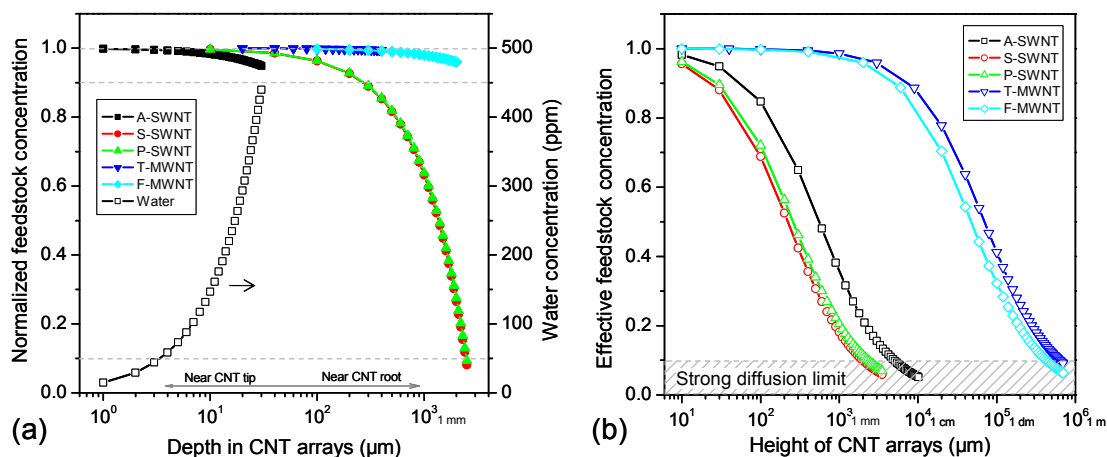


Figure 2. (a) Carbon source and by-product concentration distribution in various vertically aligned CNT arrays. A-SWNT: 30  $\mu\text{m}$  SWNT from ACCVD; S-SWNT: 2.5 mm SWNT from water-assisted super growth; P-SWNT: 2.5 mm SWNT from microwave plasma CVD; T-MWNT: 400  $\mu\text{m}$  MWNT from thermal CVD; F-MWNT: 2 mm MWNT from floating CVD; Water: water concentration inside 30  $\mu\text{m}$  SWNT from ACCVD. (b) Relationship of the CNT array height and the effective feedstock concentration at the array root, predicting the critical height above which these various CNT arrays will meet the strong diffusion resistance.

As to the error in this calculation, it is unavoidable since the influences of some factors, e.g. the bundle structure of SWNTs, the conversion rate of feedstock to CNT, tortuosity of diffusion channel (we assume it to be 1.5 in all cases) are simplified or excluded in the above discussions. However, as mentioned above, error within one order of magnitude in estimate of  $\varphi$  will not lead to a significant difference in concluding the extent of the diffusion limit. As the largest error lies on the calculation of  $D_e$ , further work on direct measurement of  $D_e$  is undergoing. Nevertheless,  $\varphi$  is helpful in understanding the role of growth parameters on the diffusion limit and the different diffusion behaviors inside SWNT and MWNT arrays.

To conclude, here we present a versatile model for one-dimensional diffusion during the root growth of aligned CNT arrays. The proposed non-dimensional modulus can be used to quantitatively evaluate the degree of the diffusion limit of feedstock, as well as byproduct molecules. The results show that, for mm-scale SWNT arrays, the feedstock concentration at the root of the array is much lower than the bulk concentration, while for mm-scale MWNTs the decreasing growth can not be attributed to a diffusion limit. The results generated from the model

agree well with experiment data. Possible strategies to grow longer CNTs in those diffusion limited processes can be revealed.

**Acknowledgement.** This work was partially supported by China National ‘863’ Program (No. 2003AA302630), China National Program (No. 2006CB0N0702), NSFC Key Program (No. 20236020), FANEDD (No. 200548), Key Project of Chinese Ministry of Education (No. 106011), THSJZ, the National center for nanoscience and technology of China (Nanoctr), and Grant-in-Aid for Scientific Research from Japan Society for the Promotion of Science (No. 19206024 and No. 19054003).

**Supporting Information Available:** Growth curves of aligned SWNT arrays from alcohol CVD and aligned MWNT arrays from floating CVD (Figure S1), evidence for the first-order reaction from ethanol to CNT in alcohol CVD (Figure S2), further explanation of equation (5), details of the calculation, and some additional discussion. This material is available free of charge via the Internet at <http://pubs.acs.org>.

## References

1. Li, W. Z.; Xie, S. S.; Qian, L. X.; Chang, B. H.; Zou, B. S.; Zhou, W. Y.; Zhao, R. A.; Wang, G. *Science* **1996**, *274*, 1701.
2. Rao, C. N. R.; Sen, R.; Satishkumar, B. C.; Govindaraj, A. *Chem. Comm.* **1998**, 1525.
3. Ren, Z. F.; Huang, Z. P.; Xu, J. W.; Wang, J. H.; Bush, P.; Siegal, M. P.; Provencio, P. N. *Science* **1998**, *282*, 1105.
4. Fan, S. S.; Chapline, M. G.; Franklin, N. R.; Tomblor, T. W.; Cassell, A. M.; Dai, H. J. *Science* **1999**, *283*, 512.
5. Murakami, Y.; Chiashi, S.; Miyauchi, Y.; Hu, M. H.; Ogura, M.; Okubo, T.; Maruyama, S. *Chem. Phys. Lett.* **2004**, *385*, 298.
6. Hata, K.; Futaba, D. N.; Mizuno, K.; Namai, T.; Yumura, M.; Iijima, S. *Science* **2004**, *306*, 1362.
7. Zhong, G. F.; Iwasaki, T.; Honda, K.; Furukawa, Y.; Ohdomari, I.; Kawarada, H. *Chem. Vapor Depos.* **2005**, *11*, 127.
8. Liu, K.; Jiang, K. L.; Feng, C.; Chen, Z.; Fan, S. S. *Carbon* **2005**, *43*, 2850.
9. Li, X. S.; Cao, A. Y.; Jung, Y. J.; Vajtai, R.; Ajayan, P. M. *Nano Lett.* **2005**, *5*, 1997.
10. Pinault, M.; Pichot, V.; Khodja, H.; Launois, P.; Reynaud, C.; Mayne-L’Hermite, M. *Nano Lett.* **2005**, *5*, 2394.
11. Zhu, L. B.; Xiu, Y. H.; Hess, D. W.; Wong, C.P. *Nano Lett.* **2005**, *5*, 2641.

12. Iwasaki, T.; Zhong, G. F.; Aikawa, T.; Yoshida, T.; Kawarada, H. *J. Phys. Chem. B* **2005**, *109*, 19556.
13. Xiang, R.; Zhang, Z. Y.; Ogura, K.; Okawa, J.; Einarsson, E.; Miyauchi, Y.; Shiomi, J.; Maruyama, S. *Jpn. J. Appl. Phys.* **2008**, submitted.
14. Zhu, L. B.; Hess, D. W.; Wong, C. P.; *J. Phys. Chem. B* **2006**, *110*, 5445.
15. Hart, A. J.; Laake, L. V.; Slocum, A. H. *Small* **2007**, *3*, 772.
16. Maruyama, S.; Kojima, R.; Miyauchi, Y.; Chiashi, S.; Kohno, M. *Chem. Phys. Lett.* **2002**, *360*, 229.
17. Maruyama, S.; Einarsson, E.; Murakami, Y.; Edamura, T. *Chem. Phys. Lett.* **2005**, *403*, 320.
18. Murakami, Y.; Maruyama, S. *Chem. Phys. Lett.* **2006**, *422*, 575.
19. Einarsson, E.; Murakami, Y.; Kadowaki, M.; Maruyama, S. *Carbon* **2007**, submitted.
20. Einarsson, E.; Kadowaki, M.; Ogura, K.; Okawa, J.; Xiang, R.; Zhang, Z. Y.; Yamamoto, T.; Ikuhara, Y.; Maruyama, S. *J. Nanosci. Nanotechnol.* **2007**, submitted.
21. Murakami, Y.; Miyauchi, Y.; Chiashi, S.; Maruyama, S. *Chem. Phys. Lett.* **2003**, *377*, 49.
22. Xiang, R.; Luo, G. H.; Qian, W. Z.; Zhang, Q.; Wang, Y.; Wei, F.; Li, Q.; Cao, A. Y. *Adv. Mater.* **2007**, *19*, 2360.
23. Levenspiel, O. *Chemical Reaction Engineering, Second Edition*, WILEY-VCH, Weinheim, Germany 1972.
24. Futaba, D. N.; Hata, K.; Yamada, T.; Mizuno, K.; Yumura, M.; Iijima, S. *Phys. Rev. Lett.* **2005**, *95*.
25. Deal, B. E.; Grove, A. S. *J. Appl. Phys.* **1965**, *36*, 3770.
26. Zhong, G. F.; Iwasaki, T.; Robertson, J.; Kawarada, H. *J. Phys. Chem. B* **2007**, *111*, 1907.
27. Zhou, W. P.; Wu, Y. L.; Wei, F.; Luo, G. H.; Qian, W. Z. *Polymer* **2005**, *46*, 12689.
28. Zhang, G. Y.; Mann, D.; Zhang, L.; Javey, A.; Li, Y. M.; Yenilmez, E.; Wang, Q.; McVittie, J. P.; Nishi, Y.; Gibbons, J.; Dai, H. J. *Proc. Natl. Acad. Sci. U. S. A.* **2005**, *102*, 16141.
29. Xiang, R.; Luo, G. H.; Qian, W. Z.; Wang, Y.; Wei, F.; Li, Q. *Chem. Vapor Depos.* **2007**, *13*, 533.
30. Xiang, R.; Luo, G. H.; Yang, Z.; Zhang, Q.; Qian, W. Z.; Wei, F. *Nanotechnology* **2007**, *18*, 415703.
31. Zhang, Q.; Zhou, W. P.; Qian, W. Z.; Xiang, R.; Huang, J. Q.; Wang, D. Z.; Wei, F. *J. Phys. Chem. C* **2007**, *111*, 14638.
32. Futaba, D. N.; Hata, K.; Namai, T.; Yamada, T.; Mizuno, K.; Hayamizu, Y.; Yumura, M.; Iijima, S. *J. Phys. Chem. B* **2006**, *110*, 8035.
33. Zhong, G. F.; Iwasaki, T.; Kawarada, H. *Carbon* **2006**, *44*, 2009.
34. Zhu, L. B.; Xiu, Y. H.; Hess, D. W.; Wong, C. P. *Nano Lett.* **2005**, *5*, 2641.

*Supporting information*

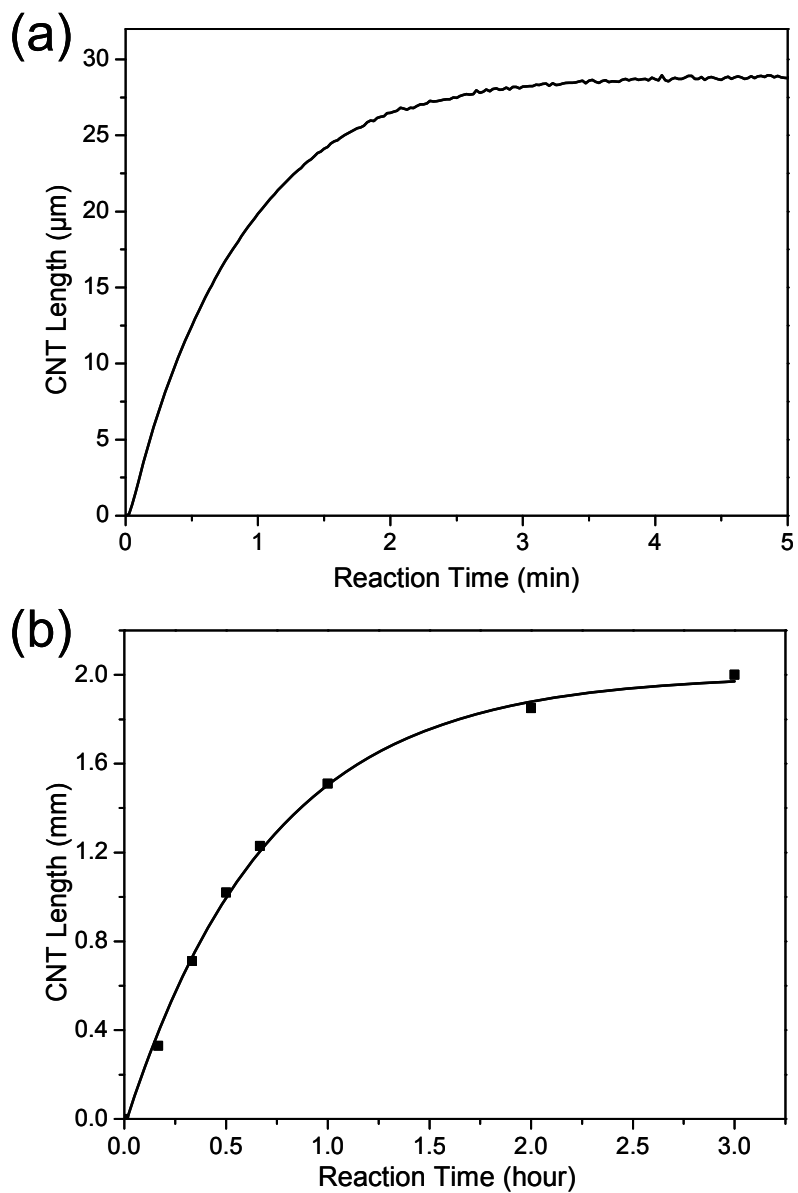


Figure S1. Time dependent growth of vertically aligned (a) SWNT arrays from ACCVD and (b) MWNT arrays from floating CVD, both of which show decelerating growth behavior over time.

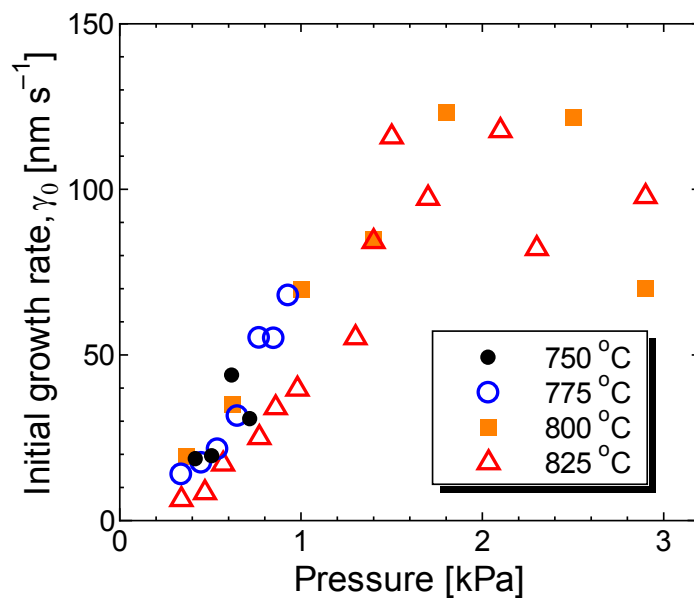


Figure S2. Relationship of initial growth rate of aligned SWNT arrays in ACCVD and the feedstock (ethanol) pressure, confirming the approximate first-order growth under different temperatures.

Further explanation of equation (5)

Depending on the values of  $\left(\frac{D_e}{k_s}\right)^2$  and  $\frac{2D_e C_0}{a}t$ ,

$L = \sqrt{\left(\frac{D_e}{k_s}\right)^2 + \frac{2D_e C_0}{a}t} - \frac{D_e}{k_s}$  can be either proportional to  $t$  or  $t^{1/2}$ .

When  $\left(\frac{D_e}{k_s}\right)^2 \ll \frac{2D_e C_0}{a}t$ ,

$$L = \sqrt{\left(\frac{D_e}{k_s}\right)^2 + \frac{2D_e C_0}{a}t} - \frac{D_e}{k_s} = \sqrt{\frac{2D_e C_0}{a}t} \propto t^{1/2};$$

When  $\left(\frac{D_e}{k_s}\right)^2 \gg \frac{2D_e C_0}{a}t$

$$L = \left( \sqrt{\left(\frac{D_e}{k_s}\right)^2 + \frac{2D_e C_0}{a}t} - \frac{D_e}{k_s} \right) \times \frac{\sqrt{\left(\frac{D_e}{k_s}\right)^2 + \frac{2D_e C_0}{a}t} + \frac{D_e}{k_s}}{\sqrt{\left(\frac{D_e}{k_s}\right)^2 + \frac{2D_e C_0}{a}t} + \frac{D_e}{k_s}} = \frac{C_0 k_s}{a} t \propto t$$

## Details of some calculations

Mean free path of molecules:

$$\lambda = \frac{RT}{\sqrt{2}\pi d^2 N_A p},$$

where  $R$  is the real gas constant,  $T$  is temperature,  $d$  the molecule diameter,  $N_A$  is Avogadro's number, and  $p$  is pressure.

Knudsen diffusion coefficient:

$$D_K = 9700r \frac{\rho}{\tau} \left( \frac{T}{M} \right)^{1/2}$$

where  $r$  is the channel diameter,  $\rho$  is the porosity of the CNT membrane,  $\tau$  is the tortuosity of diffusion channel,  $T$  is temperature, and  $M$  is molecular weight. Tortuosity  $\tau$  in our estimation was approximated to 1.5 in all cases, because it is the typical value for aligned MWNTs (ref 26). As discussed in the main text, error here will not significantly affect in the overall conclusions, i.e. judging the existence (or not) of a diffusion limit from  $\varphi$ .

Molecular diffusion coefficient:

$$D_{AB} = 0.001858T^{3/2} \frac{(1/M_A + 1/M_B)^{1/2}}{P\sigma_{AB}^2\Omega_{AB}} \left( \frac{T}{M} \right)^{1/2}$$

where  $T$  is temperature,  $M$  molecular weight,  $P$  pressure,  $\sigma$  mean molecular diameter, and  $\Omega$  collision integration. A and B stand for two components of the gas mixture in our calculation, which are the carbon source (e.g.  $C_2H_4$  or  $C_6H_{12}$ ) and a carrier gas (e.g. Ar).

Effective diffusion coefficient:

$$D_e = \left( \frac{1}{D_K} + \frac{1}{D_{AB}} \right)^{-1}$$

where  $D_K$  is the Knudsen diffusion coefficient and  $D_{AB}$  the molecular diffusion coefficient.

## Further discussion on $k_s$

In equation (5)

$$L = \sqrt{\left(\frac{D_e}{k_s}\right)^2 + \frac{2D_e C_0}{a} t} - \frac{D_e}{k_s},$$

constant  $k_s$  (no catalyst deactivation) is required to fit/predict the time-dependent growth curve. However, in most cases, catalyst activity is always diminishing, which means this equation is too ideal to be applied to a real system.

In the present method, the initial reaction constant at  $t=0$  (when there is no diffusion problem involved),  $k_{s0}$  was sufficient to exclude the diffusion limit for MWNT arrays and predict the CNT length for SWNT arrays. No complete information of catalyst decay is needed.

For the growth of mm-scale MWNT arrays, even when constant  $k_{s0}$  was used,  $\varphi$  is small and  $\eta$  is near unity. If there is some catalyst deactivation ( $k_s$  will decrease),  $\varphi$  will be even smaller. Therefore, even when the diffusion is maximized, there is no limit for these aligned MWNT arrays.

For the growth of mm-scale SWNT arrays, even if there is no catalyst deactivation (using  $k_{s0}$ ), the growth will be slowed down by the feedstock diffusion limitation. Therefore, in a real case with catalyst deactivation, SWNT arrays might not be able to grow over several mm if keeping the bulk concentration constant.